Uluslararası İleri Doğa Bilimleri ve Mühendislik Araştırmaları Dergisi
Sayı 9, S. 390-397, 10, 2025

Araştırma Makalesi

IJANSER
https://as-proceeding.com/index.php/ijanser
ISSN:2980-0811

International Journal of Advanced Natural Sciences and Engineering Researches
Volume 9, pp. 390-397, 10, 2025

Research Article

Formation of diazocyclic compounds from *o*-amino-biphenyl aromatics with nitric oxide: Investigation of the response of a fluorescent sensor containing coumarin and indoline salt to NO using DFT

Tahir Savran [*1], Şükriye Nihan Karuk Elmas [2] and İbrahim Yılmaz [1,3]

[1]*Department of Chemistry, Karamanoğlu Mehmetbey University, Karaman, Turkiye*
[2]*Department of Analytical Chemistry, Istanbul-University Cerrahpaşa, Istanbul, Turkiye*
[3]*Department of Mathematics and Science Education, Bolu Abant İzzet Baysal University, Bolu, Turkiye.*

[*]*(tahir.savran@gmail.com)*

(Received: 24 October 2025, Accepted: 26 October 2025)

(7th International Conference on Engineering and Applied Natural Sciences ICEANS 2025, October 25-26, 2025)

ATIF/REFERENCE: Savran, T., Karuk Elmas, Ş. N. & Yılmaz, İ. (2025). Formation of diazocyclic compounds from o-amino-biphenyl aromatics with nitric oxide: Investigation of the response of a fluorescent sensor containing coumarin and indoline salt to NO using DFT, *International Journal of Advanced Natural Sciences and Engineering Researches*, 9(10), 390-397.

Abstract – Reactive Oxygen Species (ROS), produced in biological reactions in living organisms, are entities that can have significant chemical effects in cellular environments. While normal levels of ROS production are positive, excessive production is negative. ROS are gasotransmitters and play important roles in physiopathological processes. Furthermore, ROS are categorized as radicals ($RO_2^{\bullet}$, –OH, $NO^{\bullet}$, and $O_2^{\bullet-}$) and non-radicals (HOCl, $ONOO^-$, $^1O_2$, H_2O_2, and O_3). ROS are associated with oxidative stress and are linked to various diseases triggered by it, such as cardiovascular disease, diabetes, and cancer. Nitric oxide ($NO^{\bullet}$) is a gaseous molecule with a very short half-life. $NO^{\bullet}$ plays a role in the regulation of nerve function, making its identification crucial. Because $NO^{\bullet}$ is a communication molecule in living organisms, the development of simple and selective fluorescent sensors for its monitoring is invaluable. Techniques for the determination of ROS include chromatography, Electron Spin Resonance, Nuclear Magnetic Resonance, Mass Spectrometric Analysis, Chemiluminescence, and Fluorescence. While these techniques are useful, the fluorescence method is superior. It is portable, requires no expertise, and is inexpensive. Consequently, the results of applying Density Functional Theory (DFT) to the sensor designed for $NO^{\bullet}$ detection are analyzed here.

Keywords – Fluorescent Probe, Coumarin, Indoline Salt, Nitric Oxide, NO, Diazo Cycle Formation, DFT.

I. INTRODUCTION

The human body can naturally produce some active species through various biochemical reactions. Reactive oxygen species (ROS) are some of these. They are chemically active molecules naturally synthesized in biological systems. The effects of ROS can be positive or negative depending on their production levels. Normal levels facilitate cellular functions such as immunity for cell development and protection. On the other hand, excessive ROS can cause genetic damage, lipid peroxidation, and potentially death [1]. ROS, as their name suggests, exhibit a higher redox activity than molecular oxygen. Some of the ROS include free radicals such as hydroperoxyl radical ($HO^{\bullet}$), superoxide radical ($O_2^{\bullet-}$),

nitric oxide radical ($NO^{\bullet}$), peroxyl radical ($ROO^{\bullet}$), hydroxyl radical ($HO^{\bullet}$), and alkoxyl radical ($RO^{\bullet}$), as well as non-radicals such as hydrogen peroxide (H_2O_2), singlet oxygen ($^1O_2$), and hypochlorous acid (HOCl) [2], [3]. The endoplasmic reticulum (ER), mitochondria, and NADPH oxidase (NOX), which synthesizes O_2^-, constitute the primary centers of endogenous ROS production [4]. Methods such as chromatography, chemiluminescence, electron spin resonance (ESR) spectroscopy, and fluorescence spectroscopy are used to detect ROS [5]. Nitric oxide ($NO^{\bullet}$), one of the three important gaseous signaling molecules, is synthesized from L-arginine by the action of $NO^{\bullet}$ synthases (NOS) [6], [7]. Furthermore, $NO^{\bullet}$ is a key biochemical messenger [8] that plays important roles in blood pressure and immune system function. It is a critical messenger molecule in immune system disorders, heart disease, and neurodegeneration. $NO^{\bullet}$, which can dilate blood vessels by acting as a neurotransmitter, is highly effective in white blood cells' destruction of tumor cells and bacteria. Determining the distribution of $NO^{\bullet}$ in the body and determining its relationship with other agents in the body will be vital in the treatment of all the problems mentioned above [9]. Various methods based on organic reactions with fluorescent probes have been reported for $NO^{\bullet}$. They can be listed the o-phenylenediamine (OPD) reaction, metal-ligand complexes, N-nitrosation of secondary amines on aromatics, formation of diazocyclic compounds from *o*-amino-3'-dimethylaminophenylaromatics, formation of the Se-NO Hantzsch bond in dihydropyridines, deamination and aromatization, conversion of thiosemicarbazide to 1,3,4-oxadiazole heterocycle, and formation of 1,2,3,4-oxatriazole from acylhydrazide and others [5], [10]–[16]. A series of fluorescent $NO^{\bullet}$ probes have been developed by attaching a $NO^{\bullet}$-recognizing moiety to organic fluorophores such as coumarin, rhodamine, BODIPY, naphthalimide, and other derivatives [17]–[21]. PET, FRET, ICT, ESIPT, and others have been reported as $NO^{\bullet}$ response mechanisms [6], [18], [22], [23].

Considering all the above-mentioned statements, the development of probes capable of $NO^{\bullet}$ determination by fluorescence spectroscopy is of great importance. In this presented study, the $NO^{\bullet}$ response of a photoinduced electron transfer (PET)-based fluorescent probe containing ortho-amino-phenyl aromatic and coumarin was investigated by considering DFT results.

II. MATERIALS AND METHOD

Theoretical calculations here were conducted using the 6–31G(d,p) basis set and the DFT/B3LYP method using the Gaussian 09W software package. Molecular energies were characterized using TD-DFT calculations [24]–[27]. In this study, a sensor containing coumarin based on the o-amino-diethylamino-biphenyl aromatic (Probe-I: (E)-2-(2-(7-((2-amino-4'-(diethylamino)-[1,1'-biphenyl]-4-yl)oxy)-2-oxo-2H-chromen-3-yl)vinyl)-3,3-dimethyl-1-pentyl-3H-indol-1-ium iodide) was envisioned and formulated, as shown in Figure 1. The designed configuration contains a fluorophore structure containing coumarin and an indoline salt. The *o*-amino-phenyl aromatic moiety, attached to this configuration via an ether bond, was designed to be the $NO^{\bullet}$-recognizing moiety (Figure 1).

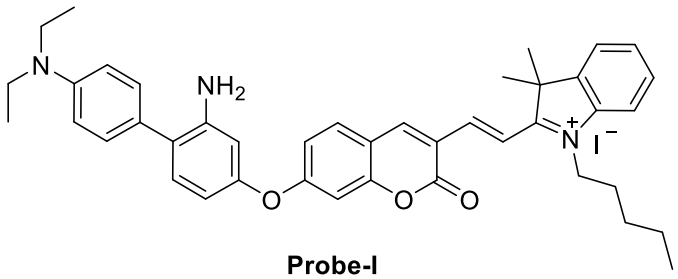

Probe-I

Fig. 1 The probe-I

A. The process route for NO determine with fluorescent chemosensors: photoinduced electron transfer (PET)

The photoinduced electron transfer (PET) system is one of the most popular chemical routes used in the design of chemical sensors. The most critical components in PET processes are aromatic

fluorophores, aliphatic amines, and methylene chain ligands. A PET-based fluorescent sensor generally composed of three components: a fluorophore (electron acceptor), a receptor (electron donor or quencher), and a chemical bond connecting the two. This system depends on a fluorophore attached to an electron-rich receptor structure, usually the amino nitrogen. The fluorophore forms the photonic processing site for excitation and emission and generates the fluorescent signal output. The receptor functions to complex with and dissociate the target. An intermediate linker keeps the fluorophore and receptor in close proximity, allowing them to exist in separate conjugated systems.

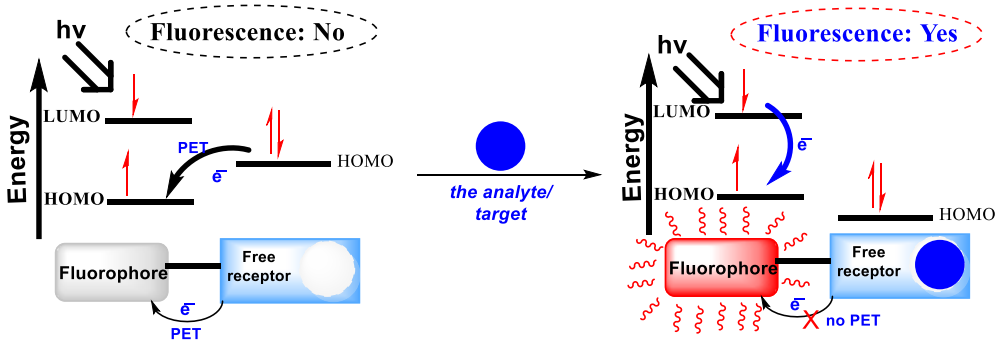

Fig. 2 The PET mechanism

When light of the appropriate wavelength is excited (which means the fluorophore is excited), intramolecular electrons are transferred from the HOMO of the receptor (electron donor) to the lower HOMO of the fluorophore (electron acceptor). As a result, fluorescence in the system is turned off. Binding an analyte/target recognition moiety reduces the energy of the receptor's HOMO, thus preventing PET transfer from the donor's HOMO to the fluorophore. This indicates that the PET process is interrupted, and the fluorescence intensity is clearly visible (a bright fluorescence emission occurs). Finally, the presence of the target is confirmed [23], [28] (Figure 2).

B. The approach for NO•: the formation of diazo-cycle compounds from o-amino-biphenyl aromatics

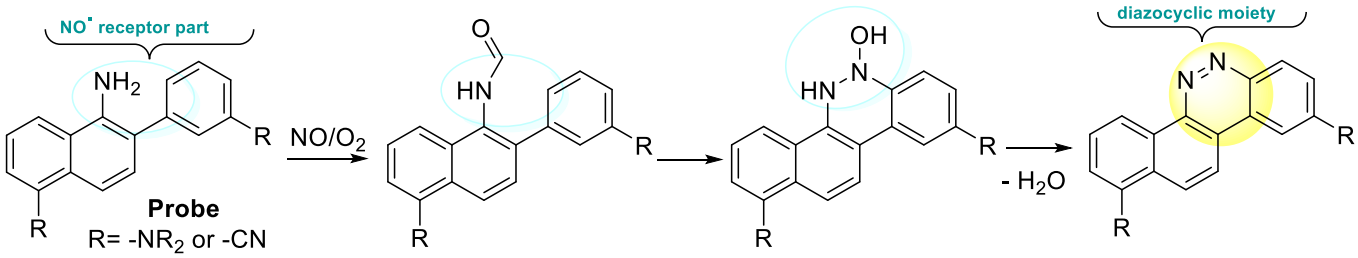

Scheme 1. The diazocyclic formation reaction strategy

The reaction method presented here involves a series of reactions that begin with the oxidation of NO• in air. The proposed molecule is expected to form a diazocyclic biphenyl system upon reaction with NO•. The cyano (-CN) or dialkylamino (-NR_2) groups are positioned to allow internal charge transfer during photoexcitation. This diazocyclic formation mechanism was theoretically demonstrated in this study to demonstrate the reactivity of the sensor compound toward NO/N_2O_3, and the structure of the product (probe-I-NO) was investigated using DFT calculations. The ring formation occurs away from the dialkylamino substituent, rather than ortho to it, likely due to steric hindrance. The reaction between probe-I and NO• requires an NO^+ donor such as NO^+ or N_2O_3. While the reaction is similar to the formation of azo compounds via the diazotization/coupling sequence, an important difference arises. Diazotization requires an acidic environment to form diazonium salts from nitrosamines. In contrast, the reaction between probe-I and NO• occurs rapidly even under basic (e.g., pH 10) or neutral (approximately pH 7) aqueous conditions, where acid-catalyzed dehydration of the initially formed nitrosamine derivative

to the corresponding diazonium salt is unlikely. This mechanism is indicative of electrophilic aromatic substitution on the electron-deficient nitrosamine, resulting in the formation of a hydroxyhydrazine derivative. This mechanism ultimately eliminates H_2O, resulting in the formation of probe-I-NO (Scheme 1) [29].

The use of fluorescent sensors based on the diazo ring formation strategy from *o*-amino-biphenyl aromatics for NO• detection has attracted significant interest in recent years (Figure 3) [6], [29]–[31].

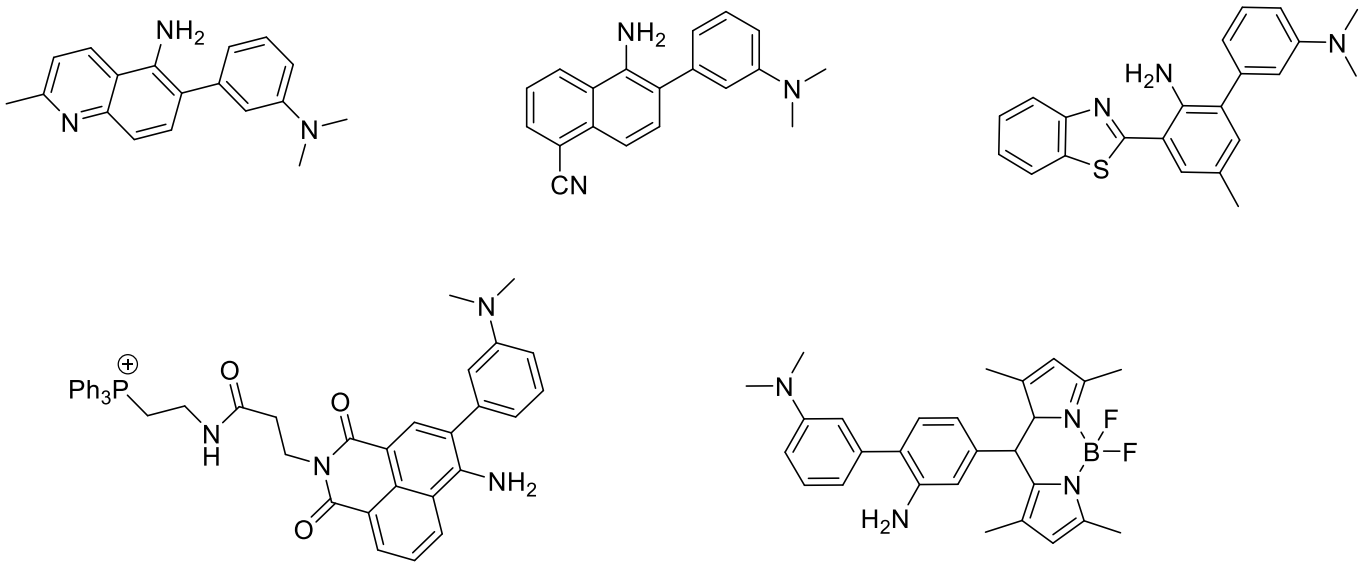

Fig. 3 Various fluorescent sensors containing *o*-amino-dialkilamino-bifenil aromatics

III. RESULTS

In the study shown in Scheme 2, the interaction phenomenon of the designed probe molecule with NO/O_2 was confirmed by giving the theoretical calculation results of the formation here.

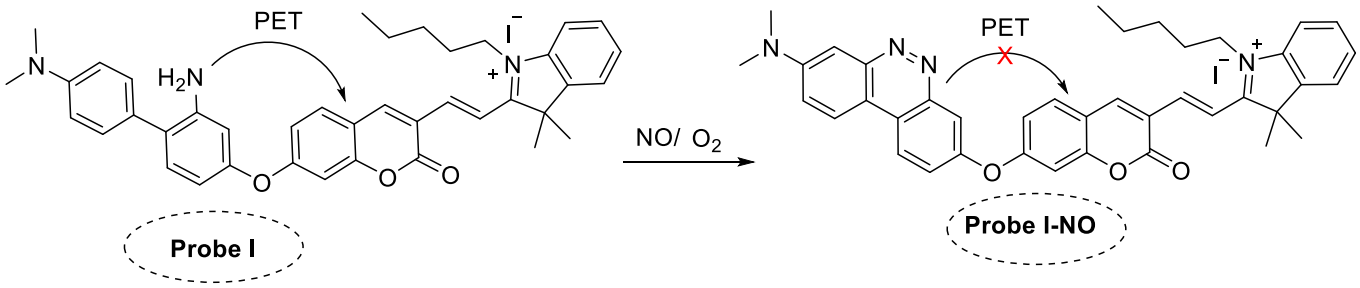

Scheme 2. The interaction pathway of the probe I designed in the work with NO/O_2

During the process, the PET mechanism was halted by the generation of diazo ring compounds as a result of the interactivity of fluorophores acquired by binding the electron-rich o-amino-biphenyl aromatic group to different molecules with NO [6], [29]–[31].

In the theoretical calculations for Probe-I, conformational analysis was performed based on the optimized geometric structure and the estimated three-dimensional structure from the molecular orbitals, and the lowest-energy optimized structure was calculated (Figure 4.(a)). Figure 4.(b) shows the molecular electrostatic potential (MEP) map obtained for Probe-I. The molecular orbitals (HOMO, HOMO-1, LUMO, and LUMO+1) for the optimized structure are presented in Figure 4.(c). The molecular orbital

values obtained for Probe-I are –7.24 eV for HOMO-1, –6.26 eV for HOMO, –5.60 eV for LUMO, and –4.03 eV for LUMO+1.

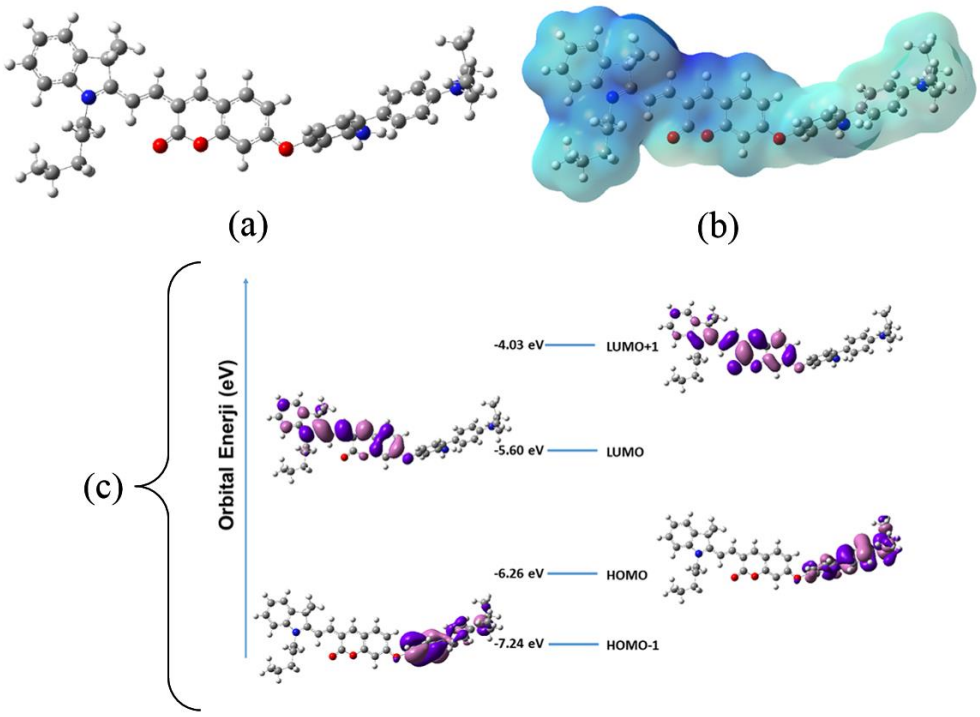

Fig. 4. Optimized geometric structure obtained for Probe-I (a), Molecular electrostatic potential (MEP) map obtained for Probe-I (b), Molecular orbitals obtained for Probe-I (c)

Conformational analysis was performed based on the optimized geometric structure of the Prob-I–NO molecule and the estimated three-dimensional structure from its molecular orbitals, and the lowest-energy optimized structure was calculated (Figure 5. (a)). The molecular electrostatic potential (MEP) map obtained for Prob-I–NO is shown in Figure 5. (b). The molecular orbitals (HOMO, HOMO-1, LUMO, and LUMO+1) for the optimized structure are presented in Figure 5. (c). The molecular orbital values obtained for Prob-I–NO are –7.44 eV for HOMO-1, 6.65 eV for 5. ((O, –5.69 eV for LUMO, and 4.12 eV for LUMO+1.

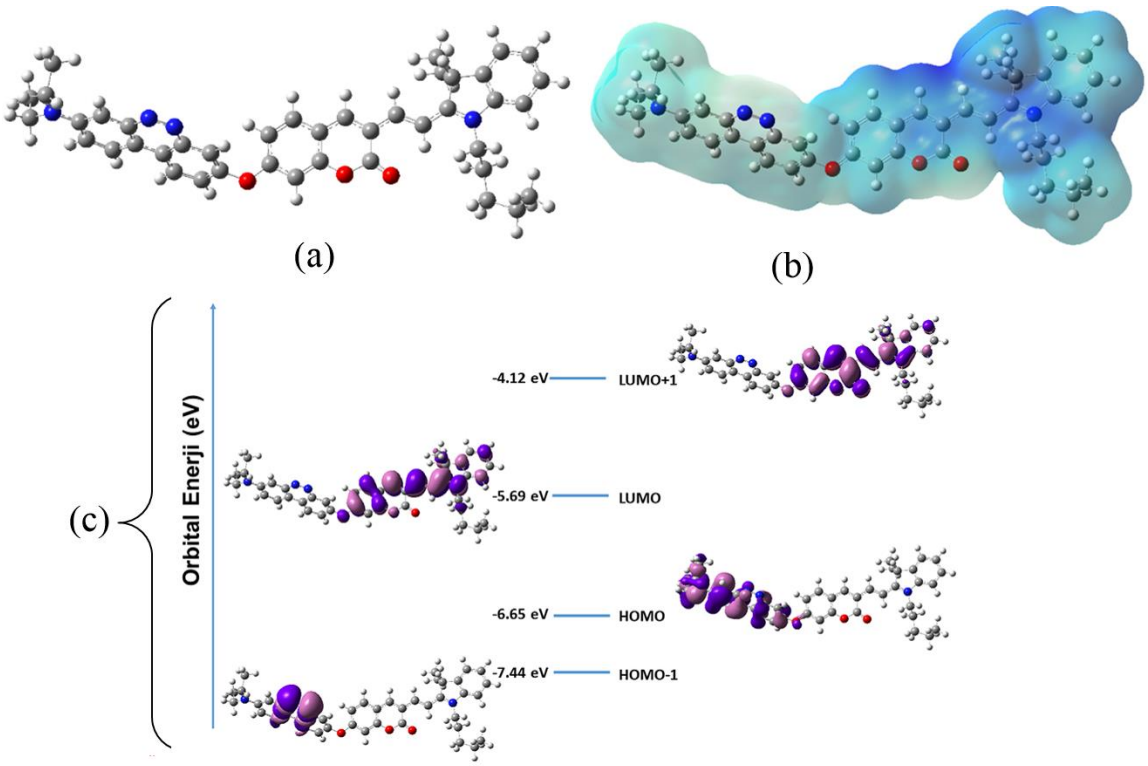

Fig. 5. Optimized geometric structure obtained for Probe-I-NO (a), Molecular electrostatic potential (MEP) map obtained for Probe-I (b), Molecular orbitals obtained for Probe-I (c)

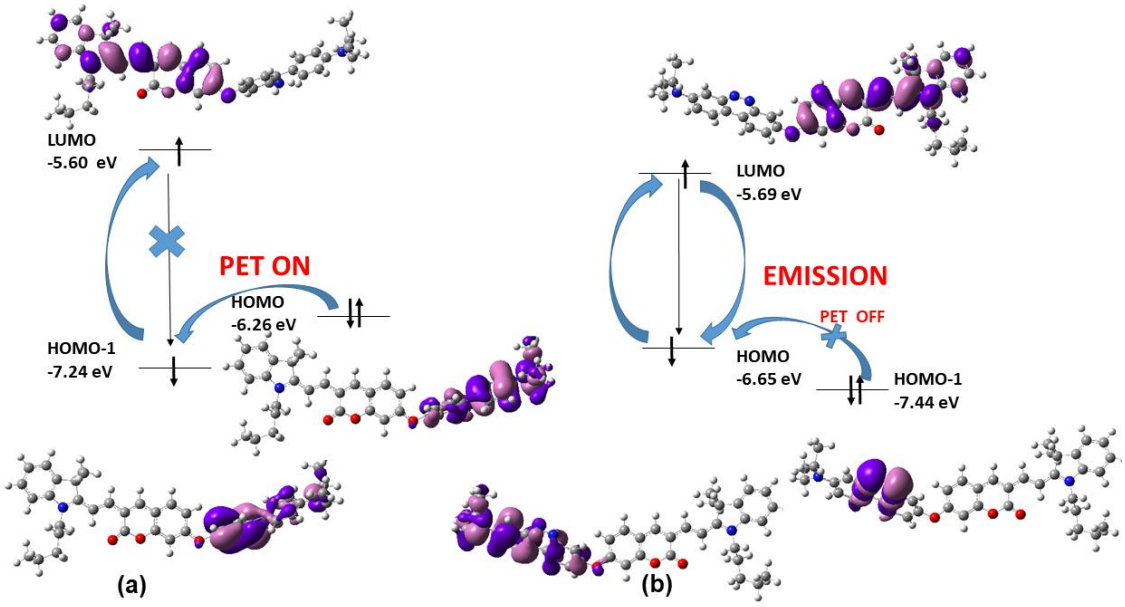

Fig. 6. Electronic transitions of Prob I (a) and Probe I–NO (b) molecules

From the electronic transitions of Prob-I and Prob-I–NO molecules, the HOMO-1 value was calculated as –7.24 eV, the LUMO value as –5.60 eV, and the GAP (energy gap between HOMO-1 and LUMO) value as 1.64 eV. The oscillator strength (f) for this transition was found to be 0.70521. From the molecular orbitals obtained for Prob-I–NO, the HOMO value was calculated as –6.65 eV, the LUMO value as –5.69 eV, and the GAP (energy gap between HOMO and LUMO) value as 0.96 eV. The oscillator strength for this transition was found to be 0.70697, and the f values obtained are among the

highest among the possible transitions. In the diazo ring approach, the diazo product is formed after treating the fluorophore obtained using the 2-amino-3'-dimethylaminobiphenyl group with nitric oxide. [6], [29]–[31]. As can be seen from Figure 6, the transitions between the ligand and the complex support the PET mechanism, in accordance with the literature [6], [29]–[31].

IV. DISCUSSION

In the diazo-cycle approach, the diazo ring product is formed after treating the fluorophore obtained using the 2-amino-3'-dimethylaminobiphenyl group with $NO^{\bullet}$. As can be seen from Figure 4, the transitions between the ligand and the complex support the PET mechanism, in accordance with the literature [6], [29]–[31].

V. CONCLUSION

In conclusion, the results of DFT computations of the $NO^{\bullet}$ interaction structure of Probe I (Probe I-NO) were investigated within the frame of this study. The acquired data were found to be compatible with the diazo cycle formation system and the PET process.

ACKNOWLEDGMENT

The authors would like to thank TÜBİTAK for supporting this work under grant number 120Z914 by the Scientific and Technological Research Council of Turkiye (TÜBİTAK).

REFERENCES

[1] L. Zuo, T. Zhou, B. K. Pannell, A. C. Ziegler, and T. M. Best, "Biological and physiological role of reactive oxygen species - the good, the bad and the ugly," *Acta Physiol.*, vol. 214, no. 3, pp. 329–348, 2015, doi: 10.1111/apha.12515.

[2] S. Bhattacharya, "Reactive Oxygen Species and Cellular Defense System," in *Free Radicals in Human Health and Disease*, 2015, pp. 1–430.

[3] A. Gomes, E. Fernandes, and J. L. F. C. Lima, "Fluorescence probes used for detection of reactive oxygen species," *J. Biochem. Biophys. Methods*, vol. 65, no. 2–3, pp. 45–80, 2005, doi: 10.1016/j.jbbm.2005.10.003.

[4] G. Saravanakumar, J. Kim, and W. J. Kim, "Reactive-Oxygen-Species-Responsive Drug Delivery Systems: Promises and Challenges," *Adv. Sci.*, vol. 4, no. 1, 2017, doi: 10.1002/advs.201600124.

[5] M. M. Tarpey, D. A. Wink, and M. B. Grisham, "Methods for detection of reactive metabolites of oxygen and nitrogen: In vitro and in vivo considerations," *Am. J. Physiol. - Regul. Integr. Comp. Physiol.*, vol. 286, no. 3 55-3, 2004, doi: 10.1152/ajpregu.00361.2003.

[6] L. Chen, D. Wu, and J. Yoon, "An ESIPT based fluorescence probe for ratiometric monitoring of nitric oxide," *Sensors Actuators, B Chem.*, vol. 259, pp. 347–353, 2018, doi: 10.1016/j.snb.2017.12.073.

[7] S. Lepiller, V. Laurens, A. Bouchot, P. Herbomel, E. Solary, and J. Chluba, "Imaging of nitric oxide in a living vertebrate using a diaminofluorescein probe," *Free Radic. Biol. Med.*, vol. 43, no. 4, pp. 619–627, 2007, doi: 10.1016/j.freeradbiomed.2007.05.025.

[8] W. Y. Hong *et al.*, "Conversion of absorption to fluorescence probe in solid-state sensor for nitric oxide and nitrite," *Org. Electron.*, vol. 14, no. 4, pp. 1136–1141, 2013, doi: 10.1016/j.orgel.2012.12.011.

[9] W. Feng *et al.*, "A 1 , 8-naphthalimide-derived turn-on fluorescent probe for imaging lysosomal nitric oxide in living cells," *Chinese Chem. Lett.*, vol. 27, pp. 1554–1558, 2016.

[10] Y. Fu, H. Li, X. Wei, and Q. Song, "BODIPY-based hydrazine as a fluorescent probe for sensitive and selective detection of nitric oxide: a new strategy," *J. Mater. Chem. B*, no. 12, pp. 3792–3795, 2019, doi: 10.1039/c9tb00626e.

[11] P. Srivastava, M. Verma, S. Sivakumar, and A. K. Patra, "A smart FRET probe exhibiting a molecular keypad lock device based on rapid detection of nitric oxide mediated by Cu2+ ion," *Sensors Actuators, B Chem.*, vol. 291, no. January, pp. 478–484, 2019, doi: 10.1016/j.snb.2019.04.093.

[12] X. X. Chen, L. Y. Niu, N. Shao, and Q. Z. Yang, "BODIPY-Based Fluorescent Probe for Dual-Channel Detection of Nitric Oxide and Glutathione: Visualization of Cross-Talk in Living Cells," *Anal. Chem.*, vol. 91, no. 7, pp. 4301–4306, 2019, doi: 10.1021/acs.analchem.9b00169.

[13] Q. Han *et al.*, "Turn-on fluorescence probe for nitric oxide detection and bioimaging in live cells and zebrafish," *ACS Sensors*, vol. 4, no. 2, pp. 309–316, 2019, doi: 10.1021/acssensors.8b00776.

[14] A. S. M. Islam, R. Bhowmick, B. Chandra Garain, A. Katarkar, and M. Ali, "Nitric Oxide Sensing through 1,2,3,4-

Oxatriazole Formation from Acylhydrazide: A Kinetic Study," *J. Org. Chem.*, vol. 83, no. 21, pp. 13287–13295, 2018, doi: 10.1021/acs.joc.8b02110.

[15] C. J. Reinhardt, E. Y. Zhou, M. D. Jorgensen, G. Partipilo, and J. Chan, "A Ratiometric Acoustogenic Probe for in Vivo Imaging of Endogenous Nitric Oxide," *J. Am. Chem. Soc.*, vol. 140, no. 3, pp. 1011–1018, 2018, doi: 10.1021/jacs.7b10783.

[16] A. S. M. Islam, R. Bhowmick, K. Pal, A. Katarkar, K. Chaudhuri, and M. Ali, "A Smart Molecule for Selective Sensing of Nitric Oxide: Conversion of NO to HSNO; Relevance of Biological HSNO Formation," *Inorg. Chem.*, vol. 56, no. 8, pp. 4324–4331, 2017, doi: 10.1021/acs.inorgchem.6b02787.

[17] D. Maiti, A. S. M. Islam, M. Sasmal, A. Dutta, A. Katarkar, and M. Ali, "A coumarin embedded highly sensitive nitric oxide fluorescent sensor: Kinetic assay and bio-imaging applications," *Org. Biomol. Chem.*, vol. 18, no. 41, pp. 8450–8458, 2020, doi: 10.1039/d0ob00567c.

[18] F. Wang *et al.*, "Acid-Promoted D-A-D Type Far-Red Fluorescent Probe with High Photostability for Lysosomal Nitric Oxide Imaging," *Anal. Chem.*, vol. 90, no. 13, pp. 7953–7962, 2018, doi: 10.1021/acs.analchem.8b00612.

[19] J. Zhang *et al.*, "A BODIPY-based dual-responsive turn-on fluorescent probe for NO and nitrite," *Dye. Pigment.*, vol. 155, no. March, pp. 276–283, 2018, doi: 10.1016/j.dyepig.2018.03.035.

[20] C. Kang, M. H. Lee, S. J. Kim, S. Y. Park, S. A. Yoon, and C. Kim, "Naphthalimide-4-(4-nitrophenyl)thiosemicarbazide: A fluorescent probe for simultaneous monitoring of viscosity and nitric oxide in living cells," *Anal. Chem.*, vol. 93, no. 10, pp. 4391–4397, 2021, doi: 10.1021/acs.analchem.0c04019.

[21] X. Y. Wang *et al.*, "A lysosomal targeted fluorescent probe based on BODIPY for monitoring NO in living cells and zebrafish imaging," *Sensors Actuators B Chem.*, vol. 383, no. February, 2023, doi: 10.1016/j.snb.2023.133592.

[22] Y. Liu, H. Fan, Y. Wen, T. Jia, Q. Su, and F. Li, "ICT-based near infrared fluorescent switch-on probe for nitric oxide bioimaging in vivo," *Dye. Pigment.*, vol. 166, no. March, pp. 211–216, 2019, doi: 10.1016/j.dyepig.2019.03.012.

[23] N. I. Georgiev, V. V. Bakov, K. K. Anichina, and V. B. Bojinov, "Fluorescent Probes as a Tool in Diagnostic and Drug Delivery Systems," *Pharmaceuticals*, vol. 16, no. 3, 2023, doi: 10.3390/ph16030381.

[24] A. D. Becke, "Density-functional thermochemistry. I. The effect of the exchange-only gradient correction," *J. Chem. Phys.*, vol. 96, no. 3, pp. 2155–2160, 1992, doi: 10.1063/1.462066.

[25] C. Lee, W. Yang, and R. G. Parr, "Development of the Colic-Salvetti correlation-energy formula into a functional of the electron density," *Phys. Rev. B*, vol. 37, no. 2, pp. 785–789, 1988.

[26] V. B. Trucks, A.M.J. Frisch, G.W., H.B. Schlegel, G.E. Scuseria, M.A. Robb, J. R. Cheeseman, G. Scalmani, "Gaussian ~ 09 Revision D.01," p. 2014, 2014.

[27] J. M. M. R. Dennington, T.A. Keith, "GaussView Version 5," p. 2009, 2009.

[28] C. Ding and T. Ren, "Near infrared fluorescent probes for detecting and imaging active small molecules," *Coord. Chem. Rev.*, vol. 482, 2023, doi: 10.1016/j.ccr.2023.215080.

[29] Y. Yang *et al.*, "A highly selective low-background fluorescent imaging agent for nitric oxide," *J. Am. Chem. Soc.*, vol. 132, no. 38, pp. 13114–13116, 2010, doi: 10.1021/ja1040013.

[30] X. Lv, Y. Wang, S. Zhang, Y. Liu, J. Zhang, and W. Guo, "A specific fluorescent probe for NO based on a new NO-binding group," *Chem. Commun.*, vol. 50, no. 56, pp. 7499–7502, 2014, doi: 10.1039/c4cc03540b.

[31] X. Zhu, J. Q. Chen, C. Ma, X. Liu, X. P. Cao, and H. Zhang, "A ratiometric mitochondria-Targeting two-photon fluorescent probe for imaging of nitric oxide: In vivo," *Analyst*, vol. 142, no. 24, pp. 4623–4628, 2017, doi: 10.1039/c7an01461a.